

Nucleon Spin and Momentum Decomposition Using Lattice QCD Simulations

C. Alexandrou,^{1,2} M. Constantinou,³ K. Hadjiyiannakou,² K. Jansen,⁴

C. Kallidonis,² G. Koutsou,² A. Vaquero Avilés-Casco,⁵ and C. Wiese⁴

¹*Department of Physics, University of Cyprus, P.O. Box 20537, 1678 Nicosia, Cyprus*

²*Computation-based Science and Technology Research Center, The Cyprus Institute, 20 Kavafi Street, Nicosia 2121, Cyprus*

³*Department of Physics, Temple University, 1925 North 12th Street, Philadelphia, Pennsylvania 19122-1801, USA*

⁴*NIC, DESY, Platanenallee 6, D-15738 Zeuthen, Germany*

⁵*Department of Physics and Astronomy, University of Utah, Salt Lake City, Utah 84112, USA*

(Received 9 June 2017; revised manuscript received 29 August 2017; published 6 October 2017)

We determine within lattice QCD the nucleon spin carried by valence and sea quarks and gluons. The calculation is performed using an ensemble of gauge configurations with two degenerate light quarks with mass fixed to approximately reproduce the physical pion mass. We find that the total angular momentum carried by the quarks in the nucleon is $J_{u+d+s} = 0.408(61)_{\text{stat}}(48)_{\text{sys}}$ and the gluon contribution is $J_g = 0.133(11)_{\text{stat}}(14)_{\text{sys}}$, giving a total of $J_N = 0.54(6)_{\text{stat}}(5)_{\text{sys}}$ that is consistent with the spin sum. For the quark intrinsic spin contribution, we obtain $\frac{1}{2}\Delta\Sigma_{u+d+s} = 0.201(17)_{\text{stat}}(5)_{\text{sys}}$. All quantities are given in the modified minimal subtraction scheme at 2 GeV. The quark and gluon momentum fractions are also computed and add up to $\langle x \rangle_{u+d+s} + \langle x \rangle_g = 0.804(121)_{\text{stat}}(95)_{\text{sys}} + 0.267(12)_{\text{stat}}(10)_{\text{sys}} = 1.07(12)_{\text{stat}}(10)_{\text{sys}}$, thus satisfying the momentum sum.

DOI: 10.1103/PhysRevLett.119.142002

Introduction.—The distribution of the proton spin among its constituent quarks and gluons has been a long-standing puzzle ever since the European Muon Collaboration showed in 1987 that only a fraction of the proton spin is carried by the quarks [1,2]. This was in sharp contrast to what one expected based on the quark model. This so-called proton spin crisis triggered rich experimental and theoretical activity. Recent experiments show that only 30% of the proton spin is carried by the quarks [3], while experiments at RHIC [4,5] on the determination of the gluon polarization in the proton point to a nonzero contribution [6]. A global fit to the most recent experimental data that includes the combined set of inclusive deep-inelastic scattering data from HERA and Drell-Yan data from Tevatron and LHC led to an improved determination of the valence quark distributions and the flavor separation of the up and down quarks [7]. The combined HERA data also provide improved constraints on the gluon distributions, but large uncertainties remain [7]. Obtaining the quark and gluon contributions to the nucleon spin and momentum fraction within lattice quantum chromodynamics (QCD) provides an independent input that is extremely crucial, but the computation is very challenging. This is because a complete determination must include, besides the valence, sea quark and gluon contributions that exhibit a large noise-to-signal ratio and are computationally very demanding. A first computation of the gluon spin was performed recently via the evaluation of the gluon helicity in a mixed action approach of overlap valence quarks on $N_f = 2 + 1$ domain wall fermions that included an ensemble with pion mass 139 MeV [8]. In this Letter, we evaluate

all of the contributions to the spin of the proton as well as the gluon and quark momentum fractions [9,10]. Such an investigation has become feasible given the tremendous progress in simulating QCD on a Euclidean four-dimensional lattice with quark masses tuned to their physical values (referred to as the physical point), in combination with new approaches to evaluate sea quark and gluon contributions that were not possible in the past [9,11–13]. This first study of valence and sea quark and gluon contributions directly at the physical point allows us to obtain complete information on the distribution of the nucleon spin and momentum among its constituents.

Computational approach.—We use one gauge ensemble employing two degenerate ($N_f = 2$) twisted mass clover-improved fermions [14,15] with masses that approximately reproduce the physical pion mass [16] on a lattice of $48^3 \times 96$ and lattice spacing $a = 0.0938(3)$ fm, determined from the nucleon mass [17]. The strange and charm valence quarks are taken as Osterwalder-Seiler fermions [18,19]. The mass of the strange quark is tuned to reproduce the Ω^- mass and the mass of the charm quark is tuned independently to reproduce the mass of Λ_c^+ , as described in detail in Ref. [17]. The strange and charm quark masses in lattice units determined through this matching are $a\mu_s = 0.0259(3)$ and $a\mu_c = 0.3319(15)$, respectively, yielding $\mu_c/\mu_s = 12.8(2)$. We note that if we instead tune to the ratio of the kaon (D meson) to pion mass m_K/m_π (m_D/m_π) for the same ensemble, we find $\mu_c/\mu_s = 12.3(1)$ [16]. Given that an extrapolation to the continuum, where the different definitions are expected to be consistent, is not carried out and the errors quoted are only statistical, this level of

agreement is very satisfactory. For the renormalized strange and charm quark masses, we find $m_s^R = \mu_s/Z_P = 108.6(2.2)(5.7)(2.6)$ MeV and $m_c^R = \mu_c/Z_P = 1.39(2)(7)(3)$ GeV, where Z_P is the pseudoscalar renormalization function determined nonperturbatively in the modified minimal subtraction scheme ($\overline{\text{MS}}$) at 2 GeV [17].

Matrix elements.—We use Ji's sum rule [20], which provides a gauge invariant decomposition of the nucleon spin as

$$J_N = \sum_{q=u,d,s,c,\dots} \left(\frac{1}{2} \Delta\Sigma_q + L_q \right) + J_g,$$

where $\frac{1}{2} \Delta\Sigma_q$ is the contribution from the intrinsic quark spin, L_q is the quark orbital angular momentum, and J_g is the gluon total angular momentum. The quark intrinsic spin $\frac{1}{2} \Delta\Sigma_q$ is obtained from the first Mellin moment of the polarized parton distribution function (PDF), which is the nucleon matrix element of the axial-vector operator. The total quark angular momentum, J_q , can be extracted by computing the second Mellin moment of the unpolarized nucleon PDF, which is the nucleon matrix element of the vector one-derivative operator at zero momentum transfer. These matrix elements in Euclidean space are given by

$$\begin{aligned} \langle N(p, s') | O_A^\mu | N(p, s) \rangle &= \bar{u}_N(p, s') [g_A^q \gamma^\mu \gamma_5] u_N(p, s), \\ \langle N(p', s') | O_V^{\mu\nu} | N(p, s) \rangle &= \bar{u}_N(p', s') \Lambda_{\mu\nu}^q(Q^2) u_N(p, s), \\ \Lambda_{\mu\nu}^q(Q^2) &= A_{20}^q(Q^2) \gamma^{\{\mu P^\nu\}} \\ &\quad + B_{20}^q(Q^2) \frac{\sigma^{\{\mu\alpha q_\alpha P^\nu\}}}{2m} \\ &\quad + C_{20}^q(Q^2) \frac{1}{m} Q^{\{\mu} Q^{\nu\}}, \end{aligned} \quad (1)$$

with $Q = p' - p$ being the momentum transfer and $P = (p' + p)/2$ the total momentum. The axial-vector operator is $O_A^\mu = \bar{q} \gamma_\mu \gamma_5 q$ and the one-derivative vector operator $O_V^{\mu\nu} = \bar{q} \gamma^{\{\mu \overleftrightarrow{D}^\nu\}} q$, where the curly brackets in O_V represent a symmetrization over pairs of indices and a subtraction of the trace. $\Lambda_{\mu\nu}^q$ is decomposed in terms of three Lorentz invariant generalized form factors $A_{20}^q(Q^2)$, $B_{20}^q(Q^2)$, and $C_{20}^q(Q^2)$. A corresponding decomposition can also be made for the nucleon matrix element of the gluon operator $O_g^{\mu\nu}$. The quark (gluon) total angular momentum can be written as $J_{q(g)} = \frac{1}{2} [A_{20}^{q(g)}(0) + B_{20}^{q(g)}(0)]$, while the average momentum fraction is determined from $A_{20}^{q(g)}(0) = \langle x \rangle_{q(g)}$ and $g_A^q \equiv \Delta\Sigma_q$, where g_A^q is the nucleon axial charge. While $A_{20}^q(0)$ can be extracted directly at $Q^2 = 0$, $B_{20}^q(0)$ needs to be extrapolated to $Q^2 = 0$ using the values obtained at a finite Q^2 .

We compute the gluon momentum fraction by considering the $Q^2 = 0$ nucleon matrix element of the operator $O_g^{\mu\nu} = 2\text{Tr}[G_{\mu\sigma} G_{\nu\sigma}]$, taking the combination $O_g \equiv O_{44} - \frac{1}{3} O_{jj}$,

$$\langle N(p, s') | O_g | N(p, s) \rangle = \left(-4E_N^2 - \frac{2}{3} \vec{p}^2 \right) \langle x \rangle_g, \quad (2)$$

where we further take the nucleon momentum $\vec{p} = 0$.

In lattice QCD, the aforementioned nucleon matrix elements are extracted from a ratio, $R_\Gamma(t_s, t_{\text{ins}})$, of a three-point function $G_\Gamma^{3\text{-pt}}(t_s, t_{\text{ins}})$ constructed with an operator Γ coupled to a quark divided by the nucleon two-point functions $G^{2\text{-pt}}(t_s)$, where t_{ins} is the time slice of the operator insertion relative to the time slice where a state with the quantum numbers of the nucleon is created (the source). For sufficiently large time separations $t_s - t_{\text{ins}}$ and t_{ins} , the ratio $R_\Gamma(t_s, t_{\text{ins}})$ yields the appropriate nucleon matrix element. To determine $B_{20}(Q^2)$, we need the nucleon matrix element for $Q^2 \neq 0$, which can be extracted by defining an equivalent ratio as described in detail in Refs. [21–23]. An extrapolation of $B_{20}(Q^2)$ is then carried out to obtain $B_{20}(0)$. We employ three approaches in order to check that the time separations $t_s - t_{\text{ins}}$ and t_{ins} are sufficiently large to suppress higher energy states with the same quantum numbers with the nucleon. These are the following. (i) Plateau method. Identify the range of t_{ins} for which the ratio $R_\Gamma(t_s, t_{\text{ins}})$ becomes time independent and perform a constant fit. (ii) Summation method. Sum $R_\Gamma(t_s, t_{\text{ins}})$ over t_{ins} , to yield $\sum_{t_{\text{ins}}} R_\Gamma(t_s, t_{\text{ins}}) = R_\Gamma^{\text{sum}}(t_s) = C + t_s \mathcal{M} + O(e^{-(E_1 - E_0)t_s}) + \dots$, where C is a constant. The matrix element \mathcal{M} is then obtained from the slope of a linear fit with respect to t_s . (iii) Two-state fit method. We perform a simultaneous fit to the three- and two-point function, varying t_{ins} for several values of t_s , including the first excited state in the fit function. If excited states are suppressed, the plateau method should yield consistent values when increasing t_s within a sufficiently large t_s range. We require that we observe convergence of the values extracted from the plateau method and, additionally, that these values are compatible with the results extracted from the two-state fit and the summation method. We take the difference between the plateau and two-state fit values as a systematic error due to residual excited states.

The three-point functions for the axial-vector and vector one-derivative operators entering the ratio $R_\Gamma(t_s, t_{\text{ins}})$ receive two contributions, one when the operator couples to the valence up and down quarks (referred to as connected) and when it couples to sea quarks and gluons (disconnected). The connected contributions are computed by employing sequential inversion through the sink [24]. Disconnected diagrams are computationally very demanding due to the fact that they involve a closed quark loop and thus a trace over the quark propagator. A feasible alternative is to employ stochastic techniques [25] to obtain an estimate of the all-to-all propagator needed for an

evaluation of the closed quark loop. For the up and down quarks, we utilize *exact deflation* [26,27] by computing the N_{ev} lowest eigenmodes of the Dirac matrix to precondition the conjugate gradient solver. Taking $N_{ev} = 500$ yields an improvement of about 20 times compared to the standard conjugate gradient method. We also exploit the properties of the twisted mass action to improve our computation using the so-called one-end trick [28,29], which yields an increase in the signal-to-noise ratio [30,31]. This also allows for an evaluation of the quark loops for all insertion time slices, and, since the two-point function is computed for all values of t_s , the disconnected three-point function is obtained for any combination of t_s and t_{ins} , allowing a thorough study of excited state effects. In addition, an improved approach is employed for $\langle x \rangle_q$, exploiting the spectral decomposition of the Dirac matrix. Within this approach, we use the lowest eigenmodes to construct part of the all-to-all propagator in an *exact* manner. This allows us to invert less stochastic sources for constant variance; hence, N_r is smaller for the $\langle x \rangle_q$ in Table I. The remaining part of the loop is calculated stochastically, with the use of the one-end trick.

For the heavier strange and charm quarks, the *truncated solver method* (TSM) [32] performs well [30,31]. In the TSM, an appropriately tuned large number of low-precision and a small number of high-precision stochastic inversions are combined to obtain an estimate of $G_s(x; x)$. We give the tuned parameters in Table I. These methods have recently been employed to compute other nucleon observables using this ensemble [33–35], as well as at higher than physical pion masses [30,31].

The three-point function of the gluon operator is purely disconnected. To overcome the low signal-to-noise ratio, we apply stout smearing to the gauge links entering the gluonic operator $O_g^{\mu\nu}$ [36]. Use of an analytic link smearing is essential for performing the perturbative computation of the renormalization. Using smearing and a total of 209 400 measurements, we obtain the bare matrix element to a few percent accuracy [11].

TABLE I. Statistics used in this calculation. t_s is the sink time separation relative to the source which is used for the connected three-point functions. N_{cfg} is the number of configurations and N_{src} the number of source positions per configuration. N_r^{HP} (N_r^{LP}) is the number of high- (low-) precision stochastic vectors used for the quark loops.

t_s/a	Connected		Observable	Disconnected			
	N_{cfg}	N_{src}		N_{cfg}	N_{src}	N_r^{HP}	N_r^{LP}
10,12,14	579	16	Light, g_A	2136	100	2250	0
16	542	88	Light, $\langle x \rangle_q$	1219	100	1000	0
18	793	88	Strange, g_A	2153	100	63	1024
			Strange, $\langle x \rangle_q$	2153	100	30	960
			Gluon, $\langle x \rangle_g$	2094	100

In Table I, we summarize the statistics used for the calculation for both quark and gluon observables.

Renormalization.—We determine the renormalization functions for the axial-vector charge and one-derivative vector operators nonperturbatively, in the regularization-invariant (RI') momentum scheme. We employ a momentum source and perform a perturbative subtraction of $O(g^2 a^\infty)$ terms [37,38]. This subtracts the leading cutoff effects yielding only a weak dependence of the renormalization factors on the renormalization scale $(ap)^2$ for which the $(ap)^2 \rightarrow 0$ limit can be reliably taken. Lattice QCD results for both the isovector and isoscalar axial charge are renormalized nonperturbatively with $Z_A^{\text{isovector}} = 0.7910(4)(5)$ and $Z_A^{\text{isoscalar}} = 0.7968(25)(91)$, respectively [35,37]. The one-derivative vector operator is nonperturbatively renormalized with $Z_{DV} = 1.1251(27)(17)$ in the $\overline{\text{MS}}$ scheme at 2 GeV [37]. The renormalization of the gluon operator is carried out perturbatively. Being a flavor singlet operator, it mixes with other operators, the quark singlet operator in particular. Owing to this mixing, appropriate renormalization conditions require computation of more than one matrix element. We perform the computation in one-loop lattice perturbation theory and use the action parameters that coincide with the ensemble of this work. To avoid the introduction of an intermediate RI-type scheme, we define a convenient renormalization prescription that utilizes both dimensional and lattice regularization results (see Ref. [11] for additional details).

The physical result of the gluon momentum fraction can be related to the bare matrix elements $\langle x \rangle_g^{\text{bare}}$ and $\langle x \rangle_q^{\text{bare}}$ using $\langle x \rangle_g = Z_{gg} \langle x \rangle_g^{\text{bare}} + Z_{gq} \sum_q \langle x \rangle_q^{\text{bare}}$, where Z_{gg} and Z_{gq} are computed to one loop. We note that the mixing coefficient Z_{gq} is a fraction of the statistical errors on our results. Therefore, for the quark momentum fractions, we renormalize with the nonperturbatively determined renormalization factor, neglecting the mixing with the gluon operator. We note that the perturbative and nonperturbative renormalization functions Z_{DV} differ by 10%, which is a much larger effect than the mixing.

In Fig. 1, we show the result of the three analyses carried out to extract the disconnected contribution to the isoscalar axial charge g_A^{u+d} and the quark momentum fraction $\langle x \rangle_{u+d}$. Taking the value at $t_s = 14a = 1.3$ fm is consistent with the result from the two-state fit and summation method, for both quantities. We take the plateau value at $t_s = 14a$ as our final result and assign as systematic error due to excited states the difference between this value and the mean value determined from the two-state fit. The same analysis is performed for the strange and charm disconnected contributions. The analysis for the valence quark contributions at lower statistics was presented in Ref. [39], and it is also followed here.

Results.—In Fig. 2, we present our results for the up, down, and strange quark contributions to the nucleon axial charge that yield the quark intrinsic spin contributions to

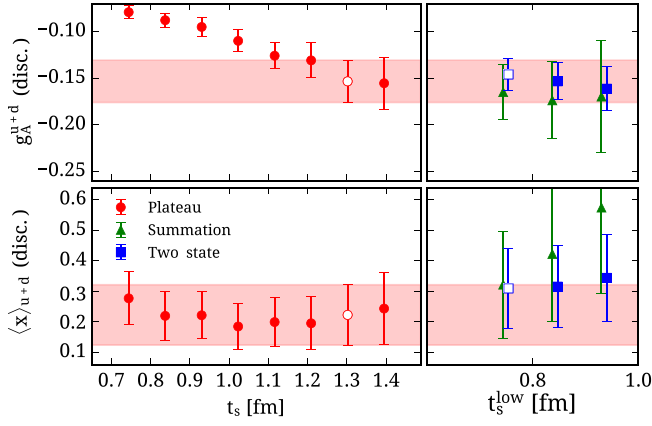


FIG. 1. The disconnected sea quark contribution (denoted by disc.) to the isoscalar axial charge (upper panel) and momentum fraction (lower panel) as a function of the sink-source time separation t_s for the plateau method (circles) and as a function of the lower time value of t_s used in the fits for the summation (green triangles) and two-state fit (blue square) methods. The open circle indicates the final value and the band its statistical error, while the open square is the value taken to determine the systematic error due to excited state contamination.

the nucleon spin. Since we are using a single ensemble, we cannot directly assess finite volume and lattice spacing effects. However, previous studies carried out using $N_f = 2$ and $N_f = 2 + 1 + 1$ twisted mass fermion (TMF) ensembles at heavier than physical pion masses for the connected contributions allow us to assess cutoff and volume effects [21,40]. In Fig. 2, we include TMF results for $N_f = 2$ ensembles at $m_\pi \sim 465$ MeV, one with lattice spacing $a = 0.089$ fm, and one with $a = 0.07$ fm, with a similar spatial lattice length L , as well as, at $m_\pi = 260$ MeV, one with $a = 0.089$ fm, and another with $a = 0.056$ fm and a similar L . At both pion masses, the results are in complete agreement as we vary the lattice spacing from 0.089 to 0.056 fm, pointing to cutoff effects smaller than our statistical errors. For assessing finite volume effects, we compare two $N_f = 2$ ensembles, both with $a = 0.089$ fm and $m_\pi \sim 300$ MeV, but one with $m_\pi L = 3.3$ and the other with $m_\pi L = 4.3$. The values are completely compatible, showing that volume effects are also within our statistical errors. To assess possible strange quenching effects, we compare in Fig. 2 results for the connected contributions using $N_f = 2$ and $N_f = 2 + 1 + 1$ TMF ensembles, both at $m_\pi \sim 375$ MeV, and find very good agreement [47]. The latter is a high statistics analysis yielding very small errors. We note, however, that the limited accuracy of the $N_f = 2$ result would still allow a quenching effect of the order of its statistical error, and only an accurate calculation using $N_f = 2 + 1 + 1$ simulations at the physical point would be able to resolve this completely. In Fig. 2, we also compare recent lattice QCD results on the strange intrinsic spin, $\frac{1}{2}\Delta\Sigma_s$, at heavier than physical pion masses and find agreement among lattice QCD results, indicating that lattice

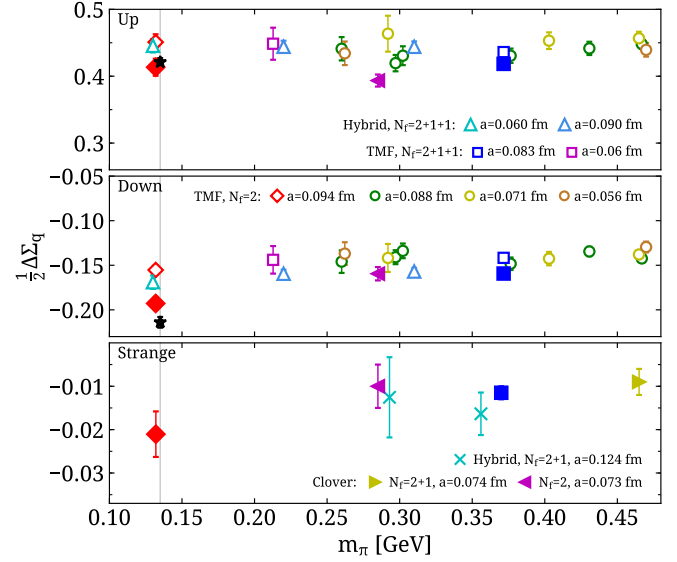


FIG. 2. The up (upper panel), down (center panel), and strange (lower panel) quark intrinsic spin contributions to the nucleon spin versus the pion mass. Open symbols show results only for the connected contributions, while filled symbols denote both connected and disconnected contributions using the same ensemble as the connected only scenario. The red diamonds are the results of this work. The circles are $N_f = 2$ results, and the squares are $N_f = 2 + 1 + 1$ [30,31,40] by ETMC. We compare this with lattice QCD results from other $O(a)$ -improved actions from Ref. [41] (the filled magenta triangle) by the QCDSF Collaboration [42] (the light blue cross), and by the CSSM/QCDSF Collaboration [43] (the yellow filled right triangle). We also show results using a hybrid action from the PNDME Collaboration [44] (the open blue triangles). The experiment is denoted by black asterisks [45,46].

artifacts are within the current statistical errors. We note, specifically, that all lattice QCD results yield a nonzero and negative strange quark intrinsic spin contribution $\frac{1}{2}\Delta\Sigma_s$. We also compute the charm axial charge and momentum fraction at the physical point, and we find that both are consistent with zero.

To determine the total quark angular momentum J_g , we need, beyond $A_{20}^q(0)$, the generalized form factor $B_{20}^q(0)$, which is extracted from the nucleon matrix element of the vector one-derivative operator for $Q^2 \neq 0$ as described in Ref. [21]. For the isovector case, we find $B_{20}^{u-d}(0) = 0.313(19)$, and for the isoscalar connected contribution $B_{20}^{u+d,\text{conn}}(0) = 0.012(20)$. We observe that the latter is consistent with zero, as is the disconnected contribution $B_{20}^{u+d,\text{disc}}(Q^2 = 0.074 \text{ GeV}^2)$. Similarly, the strange and charm $B_{20}^{s,c}(Q^2)$ values are zero, which implies that $J_{s,c} = \frac{1}{2}\langle x \rangle_{s,c}$. In what follows, we will also take the gluon $B_{20}^g(0)$ to be zero, and thus $J_g = \frac{1}{2}\langle x \rangle_g$.

Our final values for the quark total and angular momentum contributions are given in Table II. The value of $\langle x \rangle_{u-d} = 0.194(9)(11)$ is on the upper bound relative to the

TABLE II. Our results for the intrinsic spin ($\frac{1}{2}\Delta\Sigma$), angular (L), and total (J) momentum contributions to the nucleon spin and to the nucleon momentum $\langle x \rangle$, in the $\overline{\text{MS}}$ scheme at 2 GeV, from up (u), down (d), and strange (s) quarks and from gluons (g), as well as the sum of all contributions (Tot.), where the first error is statistical and the second systematic due to excited states.

	$\frac{1}{2}\Delta\Sigma$	J	L	$\langle x \rangle$
u	0.415(13)(2)	0.308(30)(24)	-0.107(32)(24)	0.453(57)(48)
d	-0.193(8)(3)	0.054(29)(24)	0.247(30)(24)	0.259(57)(47)
s	-0.021(5)(1)	0.046(21)(0)	0.067(21)(1)	0.092(41)(0)
g	...	0.133(11)(14)	...	0.267(22)(27)
Tot.	0.201(17)(5)	0.541(62)(49)	0.207(64)(45)	1.07(12)(10)

recent phenomenological value extracted in Ref. [7]. Determinations of $\langle x \rangle_{u-d}$ within lattice QCD using simulations with larger than physical pion masses have yielded larger values, an effect that is partly understood to be due to the contribution of excited states to the ground state matrix element [48]. We note that our value is in agreement with that determined by the RQCD Collaboration using $N_f = 2$ clover fermions at pion mass of 151 MeV [49], and that lattice QCD results for $\langle x \rangle_{u-d}$ and J_{u-d} for ensembles with larger than physical pion masses including ours are in overall agreement [40]. Results within lattice QCD for the individual quark $\langle x \rangle_q$ and J_q contributions are scarce. The current computation is the first one using dynamical light quarks with physical masses. A recent quenched calculation yielded values of $\langle x \rangle_{u,d}$ consistent with ours.

In Fig. 3, we show schematically the various contributions to the spin and momentum fraction. Using a different approach from ours, the gluon helicity was recently computed within lattice QCD and found to be 0.251(47)(16) [8]. Although we instead compute the gluon total angular momentum and the two approaches have different systematic uncertainties, a non-negligible gluon contribution to the proton spin is obtained within both approaches make non-negligible gluon contributions to the proton spin.

Conclusions.—In this Letter, we present a calculation of the quark and gluon contributions to the proton spin, directly at the physical point.

Having a single ensemble, we can assess only lattice systematic effects due to the quenching of the strange quark, the finite volume, and the lattice spacing indirectly from other twisted mass ensembles. A direct evaluation of these systematic errors is currently not possible and will be carried out in the future. Individual components are computed for the up, down, strange, and charm quarks, including both connected (valence) and disconnected (sea) quark contributions. Our final numbers are collected in Table II. The quark intrinsic spin from connected and disconnected contributions is $\frac{1}{2}\Delta\Sigma_{u+d+s} = 0.299(12)(3)|_{\text{conn}} - 0.098(12)(4)|_{\text{disc}} = 0.201(17)(5)$, while the total quark angular momentum is $J_{u+d+s} = 0.255(12)(3)|_{\text{conn}} + 0.153(60)(47)|_{\text{disc}} = 0.408(61)(48)$.

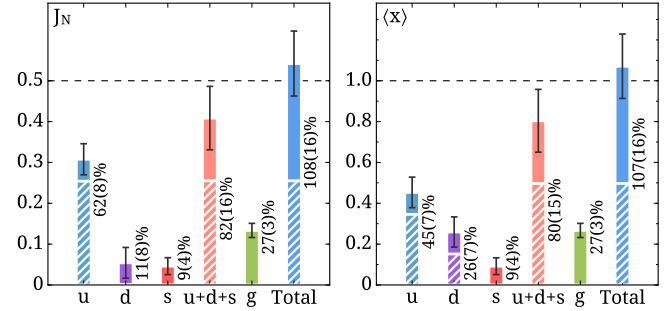


FIG. 3. (Left panel) Nucleon spin decomposition. (Right panel) Nucleon momentum decomposition. All quantities are given in the $\overline{\text{MS}}$ scheme at 2 GeV. The striped segments show valence quark contributions (connected), and the solid segments show the sea quark and gluon contributions (disconnected).

Our result for the intrinsic quark spin contribution agrees with the upper bound set by a recent phenomenological analysis of experimental data from the COMPASS Collaboration [50], which found $0.13 < \frac{1}{2}\Delta\Sigma < 0.18$. Using the spin sum, one would deduce that $J_g = \frac{1}{2} - J_q = 0.092(61)(48)$, which is consistent with taking $J_g = \frac{1}{2}\langle x \rangle_g = 0.133(11)(14)$ via the direct evaluation of the gluon momentum fraction, which suggests that $B_{20}^g(0)$ is indeed small. Furthermore, we find that the momentum sum is satisfied as $\sum_q \langle x \rangle_q + \langle x \rangle_g = 0.497(12)(5)|_{\text{conn}} + 0.307(121)(95)|_{\text{disc}} + 0.267(12)(10)|_{\text{gluon}} = 1.07(12)(10)$, as is the spin sum of quarks and gluons giving $J_N = \sum_q J_q + J_g = 0.408(61)(48) + 0.133(11)(14) = 0.541(62)(49)$, resolving a long-standing puzzle.

We thank all members of ETMC for an enjoyable collaboration, and Fernanda Steffens in particular for the fruitful discussions. We acknowledge funding from the European Union's Horizon 2020 research and innovation program under Marie Skłodowska-Curie Grant Agreement No. 642069. M. C. acknowledges financial support from the National Science Foundation under Grant No. PHY-1714407. This work used computational resources from the Swiss National Supercomputing Centre (CSCS) under Projects No. s540, No. s625, and No. s702, from the John von Neumann Institute for Computing on the Jureca and BlueGene/Q Juqueen systems at the research center in Jülich from a Gauss allocation on SuperMUC with ID No. 44060.

- [1] J. Ashman *et al.* (European Muon Collaboration), *Phys. Lett. B* **206**, 364 (1988).
- [2] J. Ashman *et al.* (European Muon Collaboration), *Nucl. Phys. B* **328**, 1 (1989).
- [3] C. A. Aidala, S. D. Bass, D. Hasch, and G. K. Mallot, *Rev. Mod. Phys.* **85**, 655 (2013).
- [4] A. Adare *et al.* (PHENIX Collaboration), *Phys. Rev. D* **90**, 012007 (2014).

- [5] P. Djawotho (for the STAR Collaboration), *Nuovo Cimento Soc. Ital. Fis.* **036C**, 35 (2013).
- [6] D. de Florian, R. Sassot, M. Stratmann, and W. Vogelsang, *Phys. Rev. Lett.* **113**, 012001 (2014).
- [7] S. Alekhin, J. Blümlein, S. Moch, and R. Placakyte, *Phys. Rev. D* **96**, 014011 (2017).
- [8] Y.-B. Yang, R. S. Sufian, A. Alexandru, T. Draper, M. J. Glatzmaier, K.-F. Liu, and Y. Zhao, *Phys. Rev. Lett.* **118**, 102001 (2017).
- [9] C. Alexandrou, M. Constantinou, K. Hadjiyiannakou, Ch. Kallidonis, G. Koutsou, K. Jansen, C. Wiese, and A. V. Avils-Casco, *Proc. Sci.*, LATTICE2016 (2016) 153 [arXiv:1611.09163].
- [10] C. Alexandrou, M. Constantinou, K. Hadjiyiannakou, C. Kallidonis, G. Koutsou, K. Jansen, H. Panagopoulos, F. Steffens, A. Vaquero, and C. Wiese, *Proc. Sci.*, DIS2016 (2016) 240 [arXiv:1609.00253].
- [11] C. Alexandrou, M. Constantinou, K. Hadjiyiannakou, K. Jansen, H. Panagopoulos, and C. Wiese, *Phys. Rev. D* **96**, 054503 (2017).
- [12] C. Alexandrou, *EPJ Web Conf.* **137**, 01004 (2017).
- [13] M. Constantinou, in *Proceedings of the 22nd International Symposium on Spin Physics (SPIN 2016), Urbana, IL, 2016* (to be published).
- [14] R. Frezzotti, P. A. Grassi, S. Sint, and P. Weisz (ALPHA Collaboration), *J. High Energy Phys.* **08** (2001) 058.
- [15] R. Frezzotti and G. C. Rossi, *J. High Energy Phys.* **08** (2004) 007.
- [16] A. Abdel-Rehim *et al.* (ETM Collaboration), *Phys. Rev. D* **95**, 094515 (2017).
- [17] C. Alexandrou and C. Kallidonis, *Phys. Rev. D* **96**, 034511 (2017).
- [18] K. Osterwalder and E. Seiler, *Ann. Phys. (Berlin)* **110**, 440 (1978).
- [19] R. Frezzotti and G. C. Rossi, *J. High Energy Phys.* **10** (2004) 070.
- [20] X.-D. Ji, *Phys. Rev. Lett.* **78**, 610 (1997).
- [21] C. Alexandrou, J. Carbonell, M. Constantinou, P. A. Harraud, P. Guichon, K. Jansen, C. Kallidonis, T. Korzec, and M. Papinutto, *Phys. Rev. D* **83**, 114513 (2011).
- [22] C. Alexandrou, M. Brinet, J. Carbonell, M. Constantinou, P. A. Harraud, P. Guichon, K. Jansen, T. Korzec, and M. Papinutto, *Phys. Rev. D* **83**, 094502 (2011).
- [23] C. Alexandrou, M. Brinet, J. Carbonell, M. Constantinou, P. A. Harraud, P. Guichon, K. Jansen, T. Korzec, and M. Papinutto, *Phys. Rev. D* **83**, 045010 (2011).
- [24] G. Martinelli and C. T. Sachrajda, *Nucl. Phys.* **B316**, 355 (1989).
- [25] K. Bitar, A. D. Kennedy, R. Horsley, S. Meyer, and P. Rossi, *Nucl. Phys.* **B313**, 377 (1989).
- [26] G. S. Bali, H. Neff, T. Düssel, T. Lippert, and K. Schilling, *Phys. Rev. D* **71**, 114513 (2005).
- [27] H. Neff, N. Eicker, T. Lippert, J. W. Negele, and K. Schilling, *Phys. Rev. D* **64**, 114509 (2001).
- [28] C. Michael and C. Urbach (ETM Collaboration), *Proc. Sci.*, LAT2007 (2007) 122 [arXiv:0709.4564].
- [29] C. McNeile and C. Michael, *Phys. Rev. D* **73**, 074506 (2006).
- [30] C. Alexandrou, M. Constantinou, V. Drach, K. Hadjiyiannakou, K. Jansen, G. Koutsou, A. Strelchenko, and A. Vaquero, *Comput. Phys. Commun.* **185**, 1370 (2014).
- [31] A. Abdel-Rehim, C. Alexandrou, M. Constantinou, V. Drach, K. Hadjiyiannakou, K. Jansen, G. Koutsou, and A. Vaquero, *Phys. Rev. D* **89**, 034501 (2014).
- [32] G. S. Bali, S. Collins, and A. Schafer, *Comput. Phys. Commun.* **181**, 1570 (2010).
- [33] A. Abdel-Rehim, C. Alexandrou, M. Constantinou, K. Hadjiyiannakou, K. Jansen, Ch. Kallidonis, G. Koutsou, and A. Vaquero Avilés-Casco, *Phys. Rev. Lett.* **116**, 252001 (2016).
- [34] C. Alexandrou *et al.*, *Phys. Rev. D* **95**, 114514 (2017).
- [35] C. Alexandrou, M. Constantinou, K. Hadjiyiannakou, K. Jansen, C. Kallidonis, G. Koutsou, and A. Vaquero Aviles-Casco, *Phys. Rev. D* **96**, 054507 (2017).
- [36] C. Morningstar and M. J. Peardon, *Phys. Rev. D* **69**, 054501 (2004).
- [37] C. Alexandrou, M. Constantinou, and H. Panagopoulos, *Phys. Rev. D* **95**, 034505 (2017).
- [38] C. Alexandrou, M. Constantinou, T. Korzec, H. Panagopoulos, and F. Stylianou, *Phys. Rev. D* **83**, 014503 (2011).
- [39] A. Abdel-Rehim *et al.*, *Phys. Rev. D* **92**, 114513 (2015); **93**, 039904(E) (2016).
- [40] C. Alexandrou, M. Constantinou, S. Dinter, V. Drach, K. Jansen, C. Kallidonis, and G. Koutsou, *Phys. Rev. D* **88**, 014509 (2013).
- [41] G. S. Bali *et al.* (QCDSF Collaboration), *Phys. Rev. Lett.* **108**, 222001 (2012).
- [42] M. Engelhardt, *Phys. Rev. D* **86**, 114510 (2012).
- [43] A. J. Chambers *et al.* (CSSM and QCDSF/UKQCD Collaborations), *Phys. Rev. D* **92**, 114517 (2015).
- [44] T. Bhattacharya, V. Cirigliano, S. D. Cohen, R. Gupta, H.-W. Lin, and B. Yoon (Precision Neutron Decay Matrix Elements (PNDME) Collaboration), *Phys. Rev. D* **94**, 054508 (2016).
- [45] A. Airapetian *et al.* (HERMES Collaboration), *Phys. Rev. D* **75**, 012007 (2007).
- [46] J. Blumlein and H. Bottcher, *Nucl. Phys.* **B841**, 205 (2010).
- [47] We find $\frac{1}{2}\Delta\Sigma_u = 0.431(11)$ and $\frac{1}{2}\Delta\Sigma_d = -0.148(7)$ for the $N_f = 2$ ensemble, which is consistent with $\frac{1}{2}\Delta\Sigma_u = 0.436(2)$ and $\frac{1}{2}\Delta\Sigma_d = -0.142(1)$ for the $N_f = 2 + 1 + 1$ ensemble.
- [48] G. S. Bali, S. Collins, M. Deka, B. Glässle, M. Göckeler, J. Najjar, A. Nobile, D. Pleiter, A. Schäfer, and A. Sternbeck, *Phys. Rev. D* **86**, 054504 (2012).
- [49] G. S. Bali, S. Collins, B. Glässle, M. Göckeler, J. Najjar, R. H. Rödl, A. Schäfer, R. W. Schiel, A. Sternbeck, and W. Söldner, *Phys. Rev. D* **90**, 074510 (2014).
- [50] C. Adolph *et al.* (COMPASS Collaboration), *Phys. Lett. B* **753**, 18 (2016).